

# Helicopter Main Rotor - Tail Rotor Interactional Aerodynamics and Related Effects on the On-Ground Noise Footprint

Stefano Melone

*Rotor Aerodynamics Senior Specialist*  
AgustaWestland, Aerodynamics Dept.  
[stefano.melone@agustawestland.com](mailto:stefano.melone@agustawestland.com)

Andrea D'Andrea

*Rotor Aerodynamics Technical Leader*  
AgustaWestland, Aerodynamics Dept.  
[andrea.dandrea@agustawestland.com](mailto:andrea.dandrea@agustawestland.com)

## ABSTRACT

Helicopter tail rotor interactional aerodynamics has been studied in the present work with special attention to the related effects on the on-ground acoustics. A medium-heavy conceptual helicopter, with an advancing-side-down tail rotor (TR), has been studied in three flight conditions in order to assess both the TR noise levels and the induced main rotor (MR) wake effects on the TR acoustics when compared to the isolated configuration. Flyover, take-off, and approach certification flight conditions have been chosen for their importance not only for the helicopter manufacturers but also for the whole community. Simulations have been carried out performing the AgustaWestland computational chain. CAMRAD J/A trim state served as input for the aerodynamic solver based on an unsteady panel method coupled with a free-wake constant vorticity contour (CVC) approach. Acoustic synthetic hemispheres, calculated according to the Farassat 1A formulation of the Ffowcs Williams-Hawkings equation, are then on-ground propagated to take into account the proper flight trajectory assessing the final TR noise contribute.

## INTRODUCTION

Helicopters are a versatile means of transport and fulfil increasingly a unique role in civil and military aviation. A serious impediment to a more widespread use of helicopters is the noise generation which, due to its characteristic impulsive and tonal content, is a source of community annoyance. With rising concern for environmental issues, helicopter noise has gained importance on par with performance, safety and reliability. The European Commission, within the CleanSky [1] research project, specifically asked under the JTI-GRC5 framework to investigate how the helicopter noise could be reduced by means of flight path optimizations minimizing the noise footprint impact on the population. Flight path optimization, anyway, cannot leave out of consideration the correct modelling of the different helicopter noise sources in the different typical flight conditions. The major helicopter noise contributors are its main rotor and tail rotor, followed by the engine and transmission. Depending on the specific flight condition one source can be predominant on the others. In the past the research has been mainly focused on isolated main rotor noise leading also to some attempts towards blade shape optimizations [1]-[4] aimed to reduce the on-ground acoustic signature especially in Blade-Vortex-Interaction (BVI) conditions, i.e., in approach flight conditions, where the tail rotor contribute is generally lower than the main rotor one. Due to the size difference, tail rotor noise is commonly erroneously considered to be less important than the much

louder main-rotor noise because, very often, the attention is focused just on approach flight conditions where the MR BVI noise is predominant. The inflow turbulence noise from a TR can be very significant because it is operated in a highly turbulent environment, ingesting wakes from upstream components of the helicopter. Interaction noise between tail-rotor and tip vortex of main-rotor becomes considerably equal to main-rotor BVI noise especially when, under certain forward flight conditions, the blade tip vortices shed by the main rotor intersect the tail rotor blades rotating at high speed in a plane perpendicular to that of the main rotor. Being mainly a perpendicular type of interaction, it results in a subjectively distinctive “burble” noise ahead of the helicopter operating in the medium-high frequency range (subjectively more annoying) [5]. In addition, the actual form that the interaction takes can vary depending on the relative timing of the main and tail rotor blade passages. In fact, the isolated convecting main rotor vortex can interact directly both with a tail rotor blade or wake. All these mutual effects complicate the flow field and make the problem of both assessing and modeling the phenomena very difficult.

Even if the tail rotor has been recognized to be an important noise source that causes early detection and gives raise to the annoyance characteristics of helicopter, due to its complex flow-field environment, the research effort in order to better understand its nature has been less extensive [3]-[8] and very often led to contradictory results. Typical are the examples of the first tests carried out on the prototypes and initial production variants of the Westland Lynx helicopter (now AgustaWestland AW159) in the 70's [5], and the wind tunnel tests carried out at the DNW on the Bo105 helicopter model scale [10][11]. In the first case, it was found that changing the TR sense of rotation from “top forward” to “top aft”, the distinctive “burble” sound produced by the helicopter was significantly reduced. This results were contradictory if compared to the Bo105 campaign where it was found that, in climbing flight and in level forward flight, the mean noise level of the helicopter with “top forward” configuration was lower than the “top aft” one. Moreover, it was found that the noise generated by the TR under the interaction of the MR was less in many cases than the TR alone. The discrepancies between the Lynx and the Bo105 cases were thought to be due to the different TR configuration between the two helicopter: the Lynx TR was located at a lower vertical position with respect to the MR hub centre than the Bo105 one. The vertical position between TR and MR is known to be one of the most important parameter affecting the interaction between the two rotors. It governs the distance and the location of the impingement of the MR wake on the TR disk plane even if it is not possible to figure out a general rule about its effects on the rotor

interactional aeroacoustics depending it also on other configuration/trim parameters. This poses the tail rotor noise and, in particular, the MR/TR interactional noise as an open field of discussion even nowadays. The proportion of main and tail rotor noise is, in fact, highly dependent on the flight condition and on the subtleties of the helicopter configuration. The sensitivity of the noise produced by a tail rotor to its vertical location with respect to the main rotor and to the specific flight condition is of particular significance, however, nowadays comprehensive studies are still rare.

Yin *et al.* in Ref. [9] first studied the MR/TR interactional problem for a generic helicopter in climb by means of a combination of an unsteady panel method and an acoustic analogy method, then Yin, in Ref [10], focused his work on the interactional effects on the aerodynamics and noise characteristics of a Bo105, firstly comparing results with the HeliNOVI Bo105 wind tunnel test data and, then, assessing the impact of the TR noise on-ground in real flight procedures. The investigation concluded that, for the studied helicopter, the TR interactional noise is most important for climb and high speed level flight and it is sensible to the TR rotational direction.

Using the same experimental database, the HeliNOVI Bo105 wind tunnel data, Brown *et al.* in Ref [11] assessed the sensitivity of the TR interactional noise to its sense of rotation and vertical displacement using the Vorticity Transport Model in conjunction with a state-of-the-art acoustic code. The results confirmed that the effect of the sense of rotation cannot be considered independently from the vertical location of the TR.

This confirms that each helicopter configuration has to be considered as a new case to be studied *ex novo* in order to understand the complex phenomena arising from the MR/TR interactions and to try to make the proper optimization actions aimed to reduce the on-ground noise impact.

The present work focuses on the ongoing activities carried out by the AgustaWestland Aerodynamics Dept. aimed to numerically simulate, from an aerodynamic and aeroacoustic point of view, both the isolated main and tail rotors, and their interaction in three certification flight conditions ranging from the high-speed flyover condition up to low-speed approach and take-off profiles. The choice to focus the attention on the interactional aeroacoustics of the three certification conditions is due, of course, to the strong interest of the helicopter manufacturers to these ones. The capability to better understand the complex phenomena behind the helicopter interactional aerodynamics in these specific flight conditions could lead industries to design quieter helicopters with margins, with respect to the certification limits, higher than the current ones with benefits not only for the manufacturer's market but also for all the community.

In the first part of the paper the used aeroacoustic computational chain will be briefly described. Then, for a conceptual helicopter with a maximum take-off weight typical for a twin-engine medium helicopter, the interactional MR/TR aerodynamic effects on on-ground propagated noise will be evaluated for the three certification flight conditions. Comparisons will be shown for the isolated and interactional TR solutions (hereafter also indicated as "coupled").

## AEROACOUSTIC COMPUTATIONAL CHAIN

Numerically predict the helicopter external noise footprint is a very hard task because it involves different

topics: flight mechanics trim procedures, accurate aerodynamic modeling of the pressure time-histories along the blade surface (i.e., accurate simulation of the rotor wake), and accurate acoustic propagation procedures. All these topics, in a sequence, constitute the aeroacoustic computational chain. This clearly means that the aeroacoustic numerical prediction can be affected by a lot of parameters and a lot of sources of uncertainty besides the effects of the simplification hypothesis behind the numerical models. In particular, the complex aerodynamic modeling of the rotor, in order to catch the pressure time-histories for each point on the blade, and the complex propagation procedure of the blades acoustic sources constitute the major effort, both in term of CPU-time and accuracy, in all the acoustic numerical prediction activities.

The numerical methodology starts with an aeromechanics comprehensive tool able to provide the main global trim parameters of the helicopter for a fixed flight condition, i.e.: fuselage pitch angle, rotor's control angles (MR collective and cyclic pitches, TR pedal), and rotor's flapping motion. To do this the selected tool is CAMRAD/JA [12]. The trim state evaluated by the comprehensive tool is, then, passed to a more accurate and advanced three-dimensional panel method (ADPANEL [13]) coupled with a state-of-the-art free-wake model. ADPANEL is able to evaluate the unsteady pressure time histories for each panel node of the blade mesh. The aerodynamic pressure time histories constitute the input database for the acoustic solver BENP [14] which, solving the classical Ffowcs Williams-Hawkings equation calculates the acoustic pressure time history, or frequency spectrum, for each node of a computational hemisphere fixed with respect to the helicopter. The last step of the chain is the on-ground propagation of the hemisphere's acoustic solution by means of the HELENA [15][16] tool according to the specified flight trajectory and flight conditions.

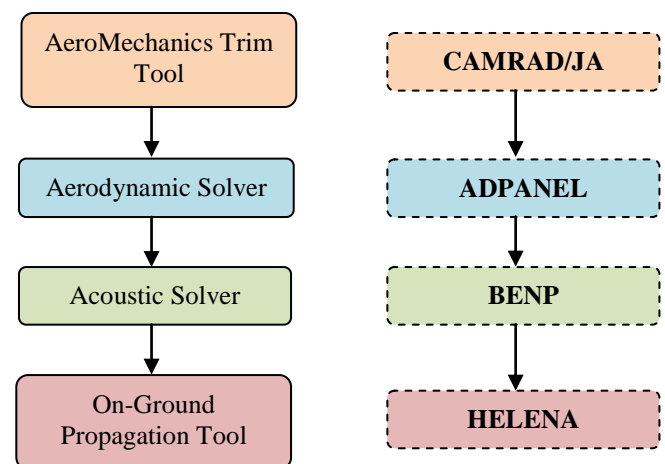


Figure 1 Aeroacoustic computational chain

### CAMRAD/JA code

The rotor aerodynamic model in CAMRAD/JA is based on lifting-line theory, using steady two-dimensional airfoil coefficient lookup tables. The induced velocity on the main rotor is calculated from the momentum theory, without a time-marching wake model and no additional unsteady effects, like dynamic stall. It results in a quick and reliable analysis tool.

## ADPANEL code

ADPANEL is a full-unstructured panel method coupled with a time-stepping full-span free wake vortex model. Present tool implements the most advanced aerodynamic features in the field of potential methods, such as the capability to represent the geometrical surfaces into unstructured-hybrid meshes, a constant vorticity contour (CVC) modeling of both rotary and fixed wing wakes, and a multi-processor implementation. Thanks to the previous features, ADPANEL is able to analyze in a quite short computational time and with detailed predictions entire helicopter and tiltrotor configurations even operating in ground effect. The wake modeling implemented in ADPANEL is composed of two parts: a “dipole buffer wake sheet”, and a set of “constant vorticity contour vortex filaments”. Buffer wake and CVC vortex filaments are used to represent the vorticity released from rotary and fixed wings for both their components, trailed and shed. The CVC free-wake modeling developed in ADPANEL allows to generate refined roll-ups and high spanwise resolution along rotor blades without enforcing an unnecessary large number of wake elements. Figure 2 shows an example of the computed CVC wake development in case of a full tiltrotor configuration operating in descent. Recent and validated “vortex dissipation laws” have been implemented in ADPANEL in order to represent the increasing of the vortex core with the time passing. Detailed information on both theory and validation of present tool can be found in [13].

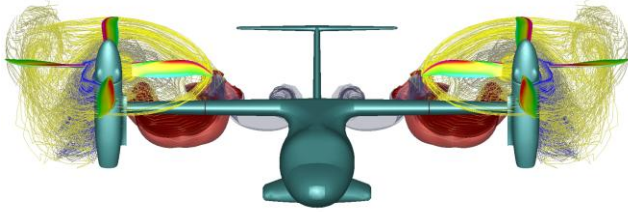


Figure 2. ADPANEL CVC wake development of the ERICA Innovative Tiltrotor in descent flight [17]

## BENP code

BENP is a state of the art acoustic tool that solves the Ffowcs Williams-Hawkings equation according to the Farassat 1A formulation to produce the acoustic pressure time history on a microphone array generally located on a computational hemisphere moving at the same velocity of the noise source. Even if the tool is able to take into account also the quadrupole noise term, for the present work, and for practical applications, just the monopole (thickness) and dipole (loading) terms are taken into account.

$$4\pi p'_T(x, t) = \int_{f=0} \left[ \frac{\rho_0 \dot{v}_n}{r(1-M_r)^2} + \frac{\rho_0 v_n \hat{r}_i \dot{M}_i}{r(1-M_r)^3} \right]_{ret} dS + \int_{f=0} \left[ \frac{\rho_0 c v_n (M_r - M^2)}{r^2 (1-M_r)^3} \right]_{ret} dS$$

$$4\pi p'_L(x, t) = \int_{f=0} \left[ \frac{p \cos \theta}{c r (1-M_r)^2} + \frac{\hat{r}_i \dot{M}_i p \cos \theta}{c r (1-M_r)^3} \right]_{ret} dS + \int_{f=0} \left[ \frac{p (\cos \theta - M_i n_i)}{r^2 (1-M_r)^2} + \frac{(M_r - M^2) p \cos \theta}{r^2 (1-M_r)^3} \right]_{ret} dS$$

The thickness contribute is evaluated starting from the 3D blade geometry taking into account also the blade pitch and flap motion; the loading term uses the unsteady pressure time histories previously evaluated by the aerodynamic solver.

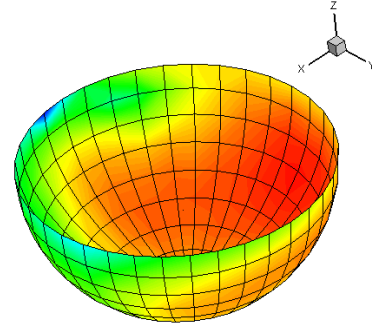


Figure 3 BENP synthetic hemisphere

## HELENA code

HELicopter Environmental Noise Analysis (HELENA) is a software platform, developed in the frame of the Friendcopter European research project, designed to provide high accuracy rotorcraft noise footprint predictions based on a database of source data which contains directivity and frequency information as a function of flight condition.

HELENA input noise source data can be obtained from flight test, wind tunnel test, comprehensive analysis tools based on the acoustic analogy, or computational aeroacoustic codes. Of course, for the work presented in this paper, a numerical database, made of synthetic hemispheres, has been used and just a limited part of the HELENA capabilities has been exploited. Each noise source is expressed as a set of sound pressure level values for the rotor blade passage frequency, and higher harmonics, as a function of spherical coordinates representing the sound directivity. All the trajectory information, helicopter trim state, atmospheric and ground parameters, microphones array complete the set of input data required by the code. Once the proper database has been, manually or automatically, chosen according to the desired flight path all the correction terms are applied if enabled. The SPL spectrum is propagated to the correct distance by computing the corresponding spherical spreading and atmospheric attenuation according to the SAE ARP866A [18] or Sutherland methods. Doppler shift and ground reflection effects, according to the Chien-Soroka model [19], are taken into account as well. The flight trajectory could be made up of a single or multiple path segments. SPL time histories for each one-third band, OASPL time history, SEL, PNLT, EPNL are the generic output variables provided by HELENA.

## PROBLEM SETUP

### Helicopter Description

A conceptual helicopter has been conceived and used for the studies presented in this paper. It is a 6500kg machine equipped with articulated MR and TR. The two rotors are oriented such as the MR is rotating counterclockwise (when viewed from above) while the TR is rotating with the advancing side down (ASD), i.e., the TR thrust is pointing starboard. For aeroacoustic purposes, for each flight condition the two rotors' centers are located in space in agreement with the trim state calculated by the CAMRAD

J/A model. This in order to ensure that the relative vertical displacement of MR and TR is, as much as possible, realistic and compliant with the flight mechanics of the aircraft, i.e., according with the fuselage pitch angle. Moreover, the TR is provided with a  $15^\circ$  of cantilever angle (see Figure 4) which allows the rotor to have not only a side force but also a vertical thrust component. A central center of gravity positioning have been assumed for the calculation of the helicopter trim state for each flight condition. The MR and TR blades have been assumed to be rigid in flap and chord modes. The blades have been equipped with AgustaWestland proprietary airfoils as well as the twist, chord and sweep distributions are taken from proprietary designs. For this reason, hereafter in the paper, some sensible data could not be shown and will be hidden without diminishing or penalizing the understanding of the presented results and their possible final contribute to the matter of research.

Both blade pitch and flap motions, as calculated by CAMRAD J/A, have been taken into account in the aeroacoustic simulations. Lead-lag motion has been neglected. In order to simplify the overall numerical procedure, the TR angular velocity has been set equal to 5 times the MR one.

In the aerodynamic and acoustic simulations no fuselage, tail, plane, fin, or engines interference effects have been taken into account. This in order to simplify the problem and to highlight just the purely aerodynamic induced noise by the MR, TR and their interaction. For sure the other sources of aerodynamic interference, like the MR/Fuselage interaction and the TR/Fin blockage, could affect the overall helicopter noise bringing to some broadband contributes and shielding effects.

In Table 1, the principal geometric and operating parameters for the MR and TR of the conceptual helicopter are summarized. In Figure 4, a sketch of MR and TR layout configuration is drawn; in dark blue the reference MR blade while in red the reference TR blade are highlighted.

	Main Rotor	Tail Rotor
No. of blades	5	4
Rotor radius	R	$R_t=0.2R$
Thrust weighted chord	$0.064R$	$0.028R$
Angular velocity	$\Omega$	$\Omega_t = 5\Omega$

Table 1 Rotors Data

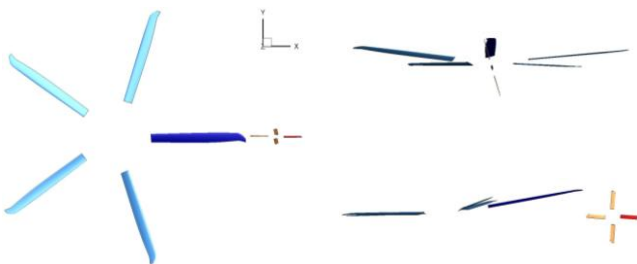


Figure 4 MR and TR layout

### Aerodynamic Modeling

As stated before, TR angular velocity has been set equal to an even number of the MR one. This choice simplify a little bit the numerical approach but, in any case, it is very close to the commonly used MR/TR ratio. In order to

maintain the computational time within acceptable values without loose in accuracy and capability to catch important aerodynamic features, the numerical simulations have been carried out with a TR azimuth discretization of  $4\text{deg}$ . As a consequence, the MR have been simulated every  $0.8\text{deg}$ . Isolated MR and TR simulations have been limited just to 4 rotor revolutions. For the simulated flight conditions, this value is enough to ensure that the rotor wake has been rolled up sufficiently to guarantee the convergence and periodicity of the final solution. For the MR/TR interactional simulations, in order to guarantee that the final solution is converged and that the TR is completely impinged by the MR wake, 20 TR rotor turns (4 MR) have been simulated after that the two rotors have been started simultaneously and impulsively from rest (see for instance Figure 5). Converged solution has been obtained for the last 5 TR turns (last MR one). The results presented in this work are related just to this time period. MR and TR blades have been modeled using 25 panels in radial direction and a total of 60 panels chordwise (30 on the upper and 30 on the lower surface) in order to properly catch wake induced load fluctuations.

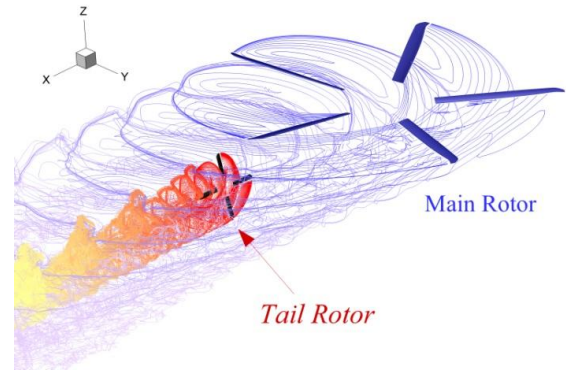


Figure 5 MR and TR wake after 20 TR turns

The comprehensive tool for trim state evaluation implements several aerodynamic models but the one chosen for the applications of this work, even if simple and reliable, is not so advanced as the one implemented in the aerodynamic tool ADPANEL. The rotor thrust coefficient provided by the latter code, for a given pitch and flap angles dataset, is very often not close to the one provided by CAMRAD J/A. This effect is clearly due to the different rotor wake modeling and related induced effects. In order to provide an aerodynamic simulation for acoustic purposes, which computed thrust is compliant with the rotorcraft trim state given by the flight mechanic tool, an adjustment to the given collective angle has been introduced until the desired rotor thrust is matched.

According to ICAO rules for acoustic certification tests, ISA+10 atmospheric conditions have been assumed.

### Acoustic Modeling

The unsteady aerodynamic pressure time histories, for each rotor blade panel, are converted into acoustic pressure time histories, according to the Farassat 1A formulation of the Ffowcs Williams-Hawkings equation, on a microphone array located on synthetic hemisphere having the same flight speed of the noise source. Thus no Doppler effect exists due to the different translational velocity between source and observer. Moreover, due to the small distance, no atmospheric attenuation effects are included. The used hemisphere has a radius of 150 meters while the observers are located every  $10\text{deg}$  of the two directivity angles, for a

total of 325 “microphones”. Both isolated MR and TR, and the interactional TR have been acoustically simulated as isolated obtaining, for each flight condition, three hemispheres to be summed up to obtain the overall noise content. For each hemisphere both acoustic pressure time history or frequency spectrum are available for each observer. The sampling rate used for the acoustic simulations has been chosen according to the aerodynamic one allowing to catch frequency contents up to 2500Hz. Higher frequencies in presence of just MR and TR are useless and time consuming because of the very low acoustic energy level associated with the MR and TR. That frequency range is, indeed, generally mainly dominated by broadband and engine noise contents which are out of the scope of the present work.

### On-Ground Propagation Modeling

The hemispheres produced by the acoustic solver, after conversion in a format suitable for HELENA, have been propagated on ground. HELENA input file just requires the frequency spectrum (blade passage frequency and higher harmonics) for each of the hemisphere observer as function of the two directivity angles. The tool is able to automatically manage both MR and TR hemisphere performing a frequency sum. Frequency sum is valid only in case the angular velocity ratio is not an even number. Because, for the purposes of the present work, MR and TR simulations have been carried out at an even angular velocity ratio, first, a time-domain sum of the two hemispheres has to be performed and, then, the final hemisphere has to be converted into the frequency domain and passed to HELENA. Spherical spreading, Doppler shift, atmospheric attenuation, and ground reflection effects are taken into account when propagating on-ground. SAE ARP866A and Chien-Soroka models have been used respectively for atmospheric and ground effects. Ground has been assumed to be made of grass as a typical airfield. This choice influences the value used for the ground resistivity required by the model. Flight trajectory and speed have been set according to ICAO rules. Moreover, microphones have been located at 1.2m above the ground. Final overhead passage time-histories are evaluate every 0.5s. All the above settings have been chosen in order to produce results and evaluate the effects of the MR/TR interactional aeroacoustics in a working frame that is close as much as possible to the certification one.

### Simulated Flight Conditions

According to ICAO rules for the helicopter certification, three flight maneuvers have been evaluated for the conceptual helicopter:

FC1: Flyover at 132kts;

FC2: Take-Off at 80kts and 15° of climb;

FC3: Approach at 80kts and -6° of descend angle.

Flight condition FC1 and FC2 are expected to be more affected by MR/TR interaction while FC3 should be mainly dominated by MR self-BVI noise.

Table 2 summarizes all the main trim parameters used for the simulations of MR and TR. It can be easily understood that in FC1 and FC2, both the relative vertical positioning between MR and TR hub centers and the TR loading, as well as the path angle, play a major role in the determination of possible interactional effects.

	FC1	FC2	FC3
$C_T$	0.07352	0.0823	0.0076
$C_{Ti}$	0.07435	0.1848	0.0023
$\theta_0$	7.62°	9.52°	3.68°
$\theta_{1C}$	2.89°	4.13°	2.31°
$\theta_{1S}$	-9.32	-7.44°	-4.84°
$\beta_0$	3.74°	4.37°	3.42°
$\beta_{1C}$	3.35°	3.29°	1.91°
$\beta_{1S}$	-0.84°	0.0°	-0.88°
$\theta_{0t}$	2.74°	10.42°	0.12°
<b>MR TPP Angle</b>	-5.95°	-15.9°	3.47°
$\Delta x$ (MR-TR)	8.398m	8.34m	8.385m
$\Delta z$ (MR-TR)	-0.225m	-0.955m	-0.514m

$$\theta = \theta_0 + \theta_{1C} \cos\Psi + \theta_{1S} \sin\Psi$$

$$\beta = \beta_0 + \beta_{1C} \cos\Psi + \beta_{1S} \sin\Psi$$

Table 2 Helicopter Trim Data

### FLIGHT CONDITION 1: FLYOVER

According to ICAO rules, flyover is performed at an aircraft speed that is a fraction of the helicopter  $V_H$  or  $V_{NE}$  whichever is less. For the scope of the present work, a flight speed of 132kts. ISA+10 atmospheric conditions have been simulated while the height above ground is fixed to 150m.

Three aerodynamic simulations have been performed: isolated MR, isolated TR, and interactional MR/TR. Isolated rotor simulations have been carried out, besides to be compared with the interactional one, also to highlight the presence, if any, of some self-BVI induced noise phenomena.

#### Flyover MR Aerodynamics (Isolated)

Figure 6 shows the isolated MR disk contour of the  $C_n M^2$  variable.  $C_n$  is the sectional force coefficient normal to the disk plane while  $M$  is the local Mach number. It is clear that, for this flight condition, no big self blade-wake interactions exist. The  $C_n M^2$  contour is fairly smooth highlighting the typical behavior of a MR at moderate-high speed level forward flight. The advancing side shows a decay of the sectional normal force while the disk results to be particularly overloaded around  $\Psi=0^\circ$ . The reversed flow region on the retreating side is clearly visible.  $C_n M^2$  contour plot results for the isolated MR are confirmed also from Figure 7 where the MR wake is drawn. Due to the disk loading and tip-path-plane angle with respect to the undisturbed velocity, the MR wake is always confined below the disk plane with no strong interactions between the blade and the wake shed by the preceding one. Figure 8 reports the  $C_n M^2$  history for the last MR turn and for two radial stations towards the blade tip. Low frequency fluctuations are just due to the cyclic combination of sectional angle of attack and Mach number.

#### Flyover TR Aerodynamics (Isolated and Coupled)

MR/TR interactional effects with respect to the isolated TR performances are clearly displayed in Figure 9 where the TR wake is shown as isolated and under the effects of the MR induction. TR interactional wake deforms considerably in comparison with the isolated one. In the same figure are also clearly visible the points of MR/TR wake-wake orthogonal interaction. Due to the helicopter trim state, i.e., the relative vertical displacement between the two rotors, MR tip vortices remain confined within the retreating side region of the TR disk.

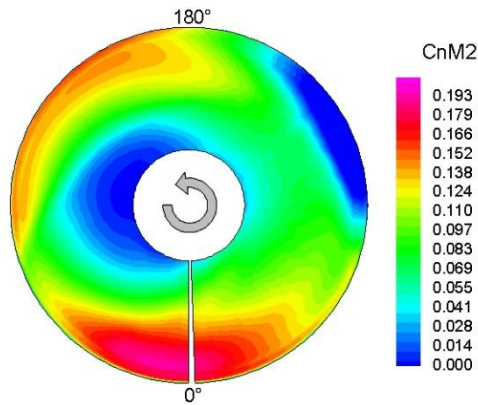


Figure 6. Contour plot of  $C_n M^2$  distribution on MR disk in FlyOver condition (last turn)

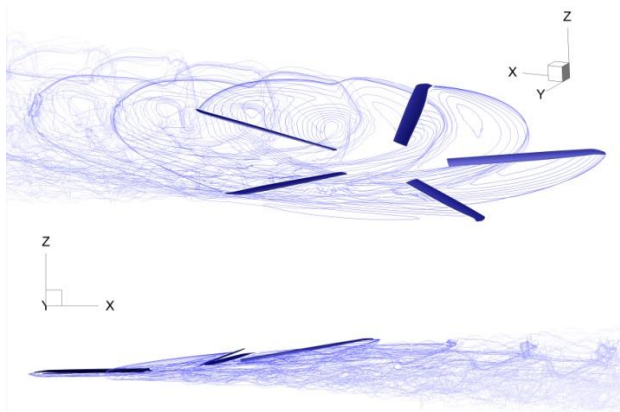


Figure 7. Isolated MR wake in Flyover

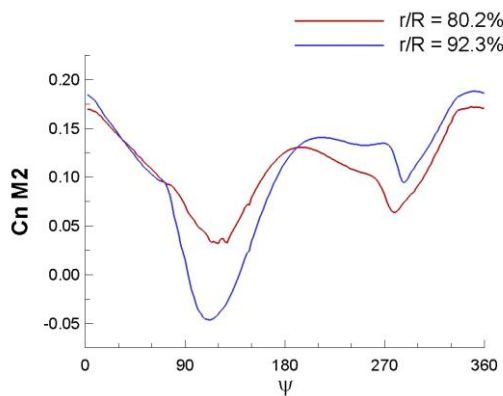


Figure 8.  $C_n M^2$  history for the isolated MR in Flyover

Due to the lower local Mach number, this should cause weaker interactions between TR blades and MR wake with respect to the case where the MR wake impingement would be confined within the advancing sideregion of the disk. The induced MR wake effects alter not only the local TR aerodynamics but also its global performance, i.e., its thrust capability. It was found that the same TR thrust coefficient, required in flyover to satisfy the helicopter trim state, can be obtained in case of MR/TR interaction with a little bit higher pedal angle ( $+0.5^\circ$ ) than the isolated TR.

The unsteadiness associated with the rotors' interactions causes the blade sectional loads changing during the TR revolutions and displaying a time periodicity equal to the MR period of revolution.

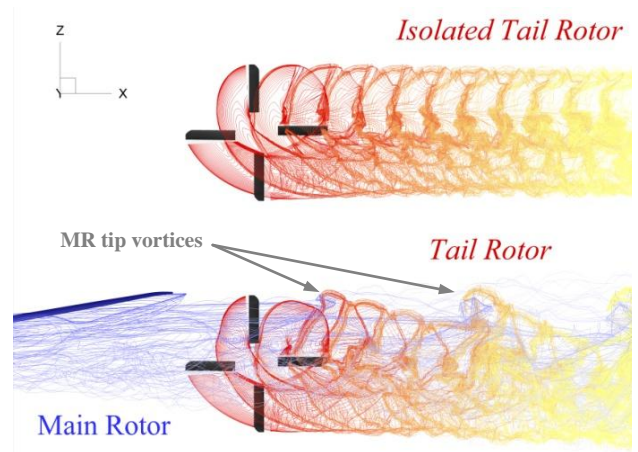


Figure 9. Isolated TR and coupled TR wake in Flyover

Comparison of  $C_n M^2$  and  $d(C_n M^2)/d\Psi$  contour plots on the TR disk, for both the isolated and the coupled case, are shown in Figure 10 and Figure 11 respectively. Just the last turn is displayed for the isolated case while the last five turns are shown for the interactional one. Both figures highlight that interesting modifications occur on the disk loading when the TR is coupled to the MR. During the isolated TR operations, several self-BVIs occur between  $\Psi=0^\circ$  and  $\Psi=90^\circ$ . In medium-high speed forward flight, in fact, the anti-torque contribute is split between the TR and the vertical fin and, thus, the TR is not required to produce a large amount of side force. This implies that the TR disk loading is not so high and, of course, the wake induced velocities are such that, combined with the free stream velocity, the rotor wake tends to remain within the disk plane interacting with the blades and causing self-BVIs. For the coupled TR, instead, the MR wake tends to alter the way the TR blades interact with the wake shed by the preceding ones. In this way the TR self-BVIs phenomena are diminished, especially around  $\Psi=45^\circ$ . Between  $\Psi=180^\circ$  and  $\Psi=270^\circ$  on the retreating side of the coupled TR, instead, the interactional effects trigger loads fluctuations that in any case seem to be weaker than a typical BVI phenomenon. The same phenomena seem to occur on both the rotors between  $270^\circ$  and  $360^\circ$  but with just a light phasing.  $C_n M^2$  time histories for the isolated and coupled TR, for three radial stations, are shown in Figure 12. The reduction of the TR self-BVI phenomena due to the MR wake effects is shown as well as the presence of new low frequency sectional load oscillations between  $180^\circ$  and  $270^\circ$ . A parallel self-BVI seems to occur between  $\Psi=15^\circ$  and  $\Psi=30^\circ$  extending all over the blade span.

#### Flyover MR Acoustics (Isolated)

MR and TR have quite completely different acoustic behaviour both in terms of sound levels and directivity. Hemispheres are the useful way to show and compare them for a number of observers located at the same distance from the source and moving at the same velocity. In Figure 13 the Over-All-Sound-Pressure-Level (OASPL) is shown for the isolated MR hemisphere. Both OASPL in dB and dB(A) contours are drawn. The A-weighting filter tends to fairly reproduce in a simple fashion the response of the human ear to an acoustic disturbance filtering the low frequency contents. Now, because OASPL-dB is mainly affected by low frequency contributes, it could be misleading just comparing MR and TR (both isolated and interactional) acoustic

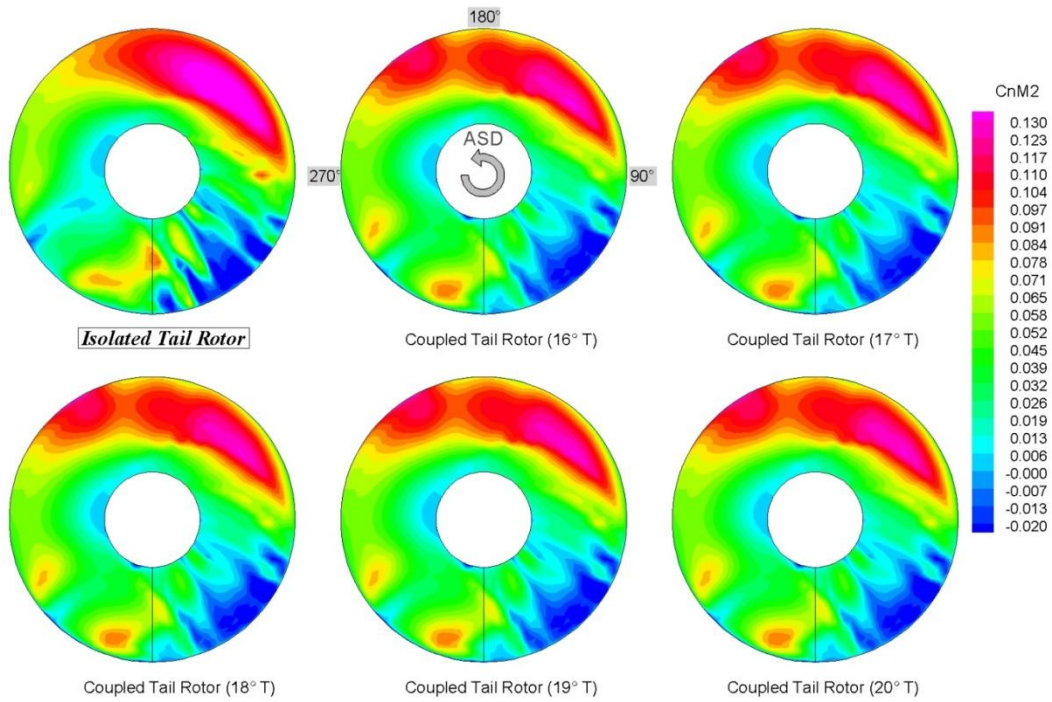


Figure 10. Contour plot of  $C_n M^2$  distribution on TR disk in FlyOver. Isolated TR (last turn) vs. Coupled TR (last five turns)

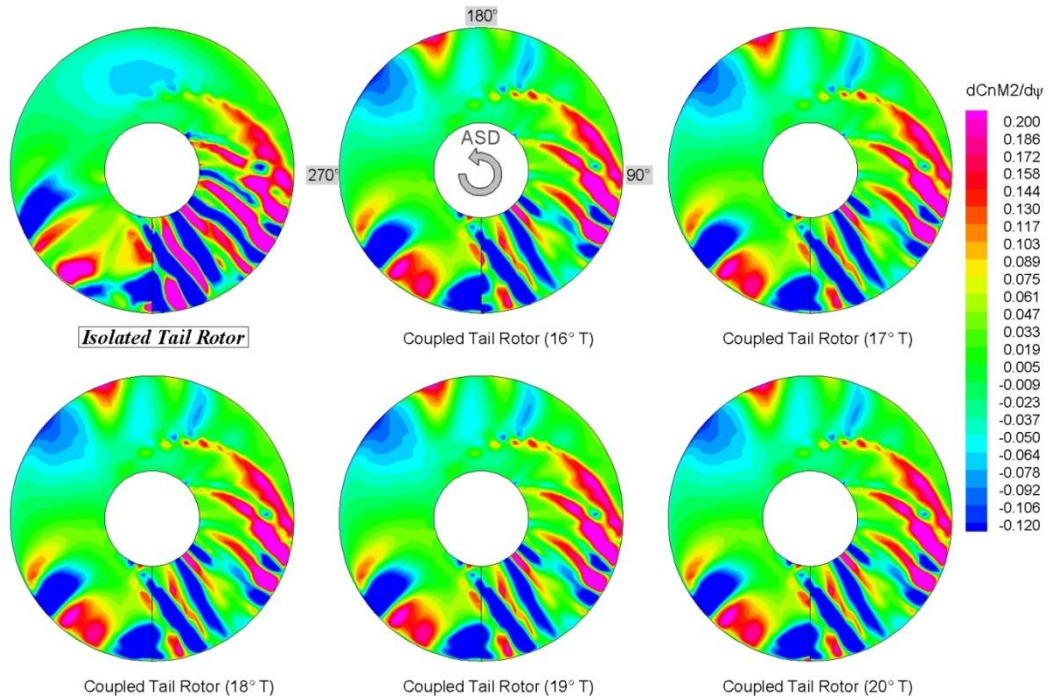


Figure 11. Contour plot of  $dC_n M^2/d\psi$  distribution on TR disk in FlyOver. Isolated TR (last turn) vs. Coupled TR (last five turns)

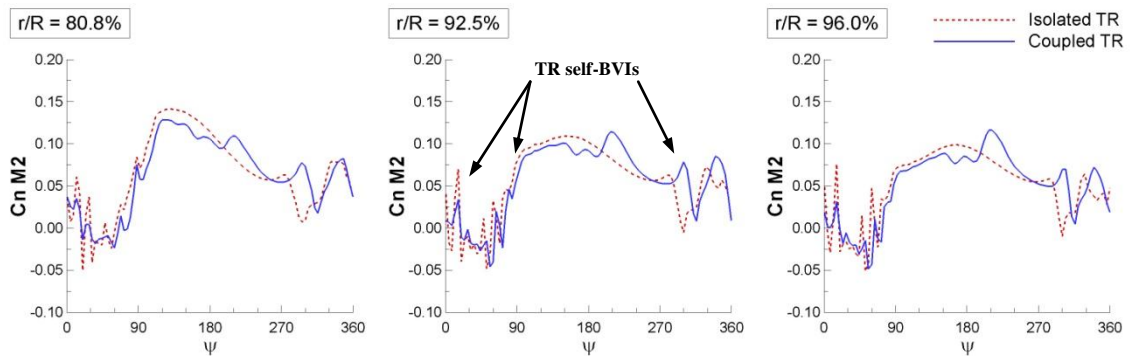


Figure 12. Sectional  $C_n M^2$  distributions comparison in FlyOver on last Tail rotor turn. Isolated TR (dashed) vs. Coupled TR (solid)

behaviour only in terms of dB without any kind of filtering. This is even more important when the final goal of the research is try to assess the rotor acoustic performances according to the certification rules. Moreover, for the calculation of the hemispheres, both thickness (monopole) and loading (dipole) terms are taken into account. For sure, for a MR, the low frequency thickness noise can affect the helicopter detectability far away from the source because it mainly propagates on the disk plane. For the TR, instead, thickness contribute mainly propagates toward the ground and due to the higher TR blade passage frequency, its effects could affect the proximity on-ground noise footprint. In Flyover, the MR mainly propagates below and on the front of the disk plane (see Figure 13 left). The flyover MR hemisphere contour in dB(A), in any case, shows that its overall contribute is highly diminished by the A-filtering confirming that, for this flight condition, no important high-frequency phenomena, such as self-BVI, occurs.

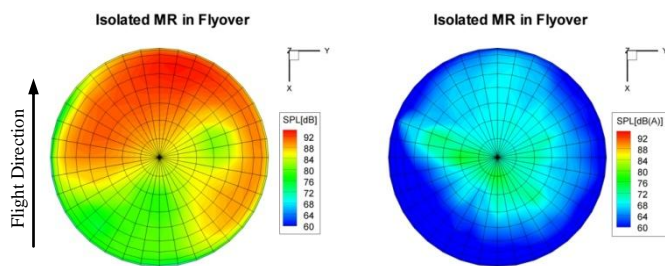


Figure 13 OASPL-dB and OASPL-dB(A) contours on the isolated MR hemisphere in Flyover

#### Flyover TR Acoustics (Isolated and Coupled)

Figure 14 shows the numerical hemispheres for both the isolated TR and for the TR under the interactional aerodynamics of the MR. TR directivity is mainly toward the port side of the helicopter and is affected by the 15° of TR cantilever angle. It is clear that, in this case, the interaction between the MR tip vortices and the TR blades has positive effects on the reduction of the TR noise. The isolated TR self-BVI phenomena observed in Figure 10 (top-left) and Figure 12 have been strongly reduced or partially cancelled by the deformation of the TR wake after the interaction with the MR one. In any case, the higher frequency contents of the TR and, thus, its very important annoying effects on the human perception in flyover conditions, are clearly visible comparing the dB and dB(A) hemispheres. The acoustic time histories for the points marked as “MAX” on the TR hemispheres are displayed, for one rotor revolution, in Figure 15. For each quarter of period, two strong and close self-BVI impulses are visible for the isolated TR while the interactional one displays the same peaks but retarded in time and with lower amplitude.

Figure 16 confirms that, in flyover, the isolated TR displays higher SPL values than the interactional TR. Moreover, it can be noticed that, the latter shows important noise contents not only at the prescribed rotor frequencies, i.e., the blade passage frequency and higher harmonics, but also at intermediate frequencies. This means that, due to the MR-TR wake interactions, the whole acoustic energy content of the interactional TR is spread more continuously all over the frequency spectrum than the isolated one.

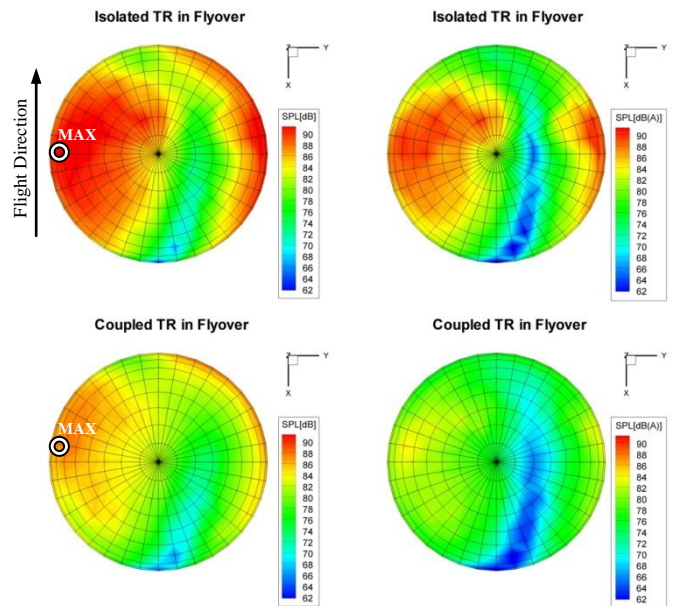


Figure 14 OASPL-dB and OASPL-dB(A) contours on the isolated and coupled TR hemispheres in Flyover

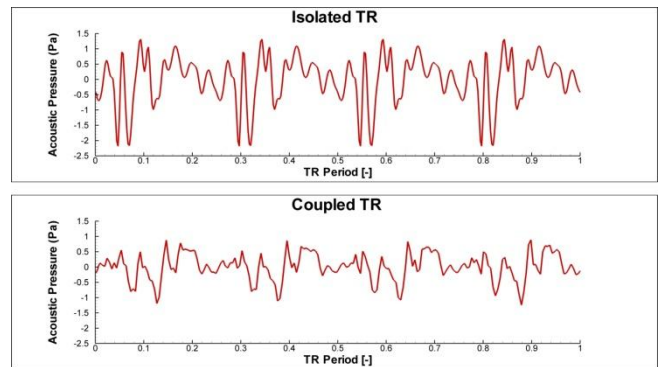


Figure 15 TR acoustic pressure time-histories for the points marked as “MAX” in Figure 14: isolated TR (upper) vs coupled TR (lower) in Flyover

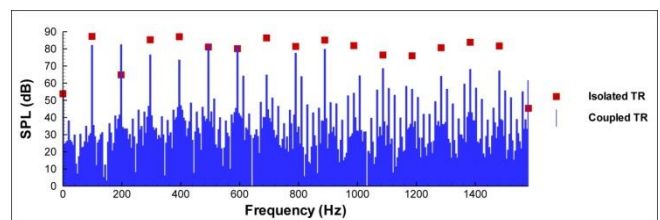


Figure 16 TR acoustic frequency spectrum in Flyover for the points marked as “MAX” in Figure 14

#### Flyover On-Ground Propagation

On-ground propagation of the acoustic hemispheres of the isolated MR, isolated TR, and interactional TR highlights some important conclusions. ICAO rules prescribe that flyover passage is performed at 150m of height above ground with the measurements performed over three microphones located orthogonally to the flight path and at 150m of relative distance between them. Time history of the OASPL-dB for the certification central microphone, drawn in Figure 17

(upper), shows that, in flyover, MR would be the major noise contributor especially at some distance from the microphone. Moreover, the effect of the different noise directivity pattern that causes a delay between MR and TR OASPL peaks is also clear. MR+TR OASPL-dB curves highlight the relative importance of the TR with respect to the MR and the big differences arising if the TR is considered as isolated or coupled. The isolated TR, in correspondence of the overhead microphone passage, seems to be as important as the MR while the interactional TR contribute is of second order. The intense self-BVI phenomena occurring on the isolated TR, indeed, give rise to a 6dB of max-OASPL difference with respect to the interactional TR. This “objective” scenario, in any case, is completely altered when the OASPL time histories are compared in terms of dB(A), i.e., in a more “subjective” way taking into account the noise perception of the human ear. Figure 17 (lower), shows that the sum contribute of MR and TR is completely dominated by the TR, even far away from the source, due to the higher TR frequencies than the MR ones. Moreover, also the different aeroacoustic behaviour of the isolated TR with respect to the interactional one is amplified and made more evident: the isolated TR exhibits a max-OASPL dB(A) value that is roughly 8dB(A) greater than the one of the interactional TR. A-weighting tends to preserve more the higher and louder frequencies associated to the self-BVI phenomena occurring on the isolated TR.

coupled TR, and the relative importance between MR and TR contributes in flyover (see Figure 19). This results, thus, imply that TR noise contribute in flyover cannot be neglected when an indication of the complete machine noise is required and attention has to be paid taking into account the interactional aeroacoustics of MR and TR.

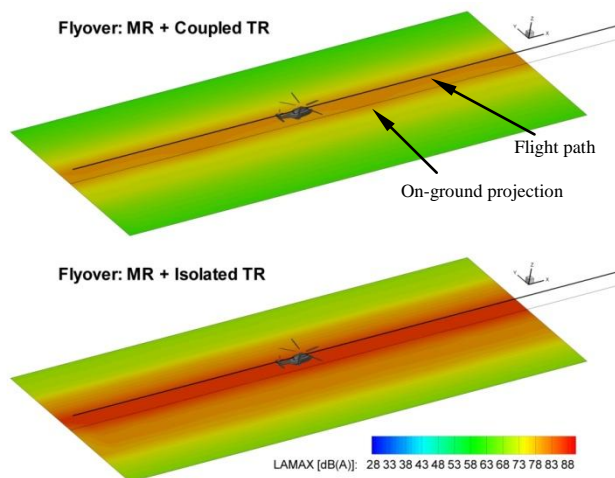


Figure 18 Max-OASPL-dB(A) contour plots in Flyover: comparison between isolated and coupled TR

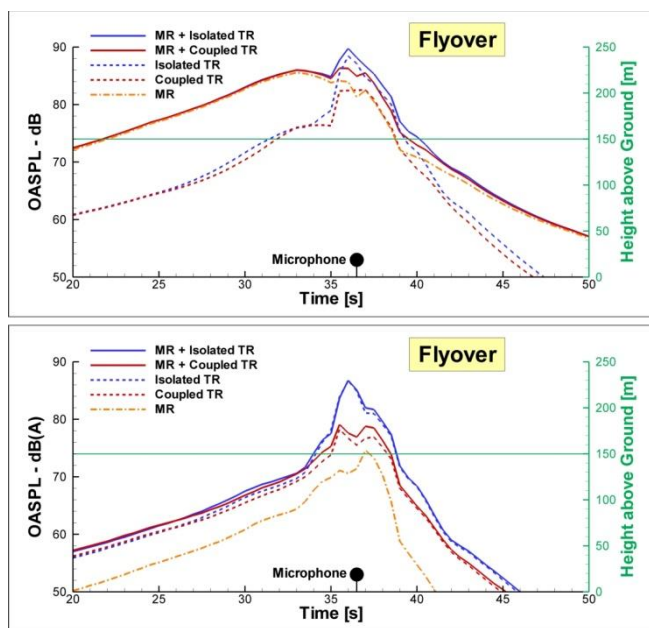


Figure 17 OASPL-dB and OASPL-dB(A) time-histories for the central microphone in Flyover

The on-ground contour plots of the max OASPL-dB(A) for the sum of MR and TR (both isolated and coupled) are shown in Figure 18.

Effective-Perceived-Noise-Level (EPNL-dB) is the noise synthetic index used for certification purposes. It should fairly summarize the human noise perception taking into account not only the frequency content but also the duration of the 10-dB-down period of the noise curve. Like the OASPL-dB(A) curve, the synthetic EPNL value, even if evaluated just starting from numerical simulations, highlights and confirms both the differences between the isolated and

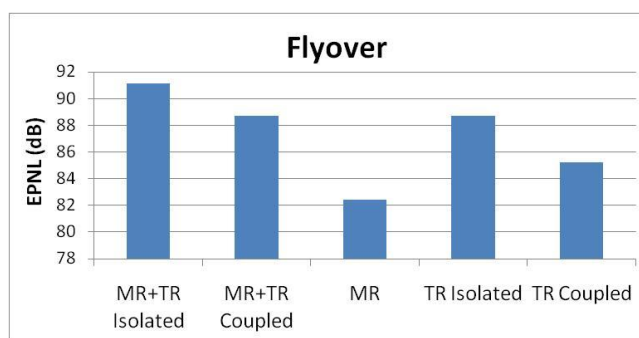


Figure 19 EPNL estimation in Flyover

## FLIGHT CONDITION 2: TAKE-OFF

ICAO rules state that Take-Off must be performed at the best rate of climb speed ( $V_y$ ) and maximum power allowable with the specified flight condition. The climb path angle must be given by the best rate of climb and  $V_y$ . For the conceptual helicopter here defined, the  $V_y$  is equal to 80kts while the climb angle is set to 15°.

### MR Aerodynamics (Isolated)

Like flyover, even take-off is characterized by low frequency sectional load variations. During take-off the MR disk results to be very loaded, i.e., a very high thrust coefficient is produced. This gives rise to very high induced velocities that, coupled to the rotor tip-path-angle and helicopter climb angle, causes that the MR wake is always well below the disk plane avoiding any interaction with the rotor blades (Figure 20).  $C_n M^2$  contour (Figure 21) and azimuth histories for two radial stations (Figure 22) confirm this statement.

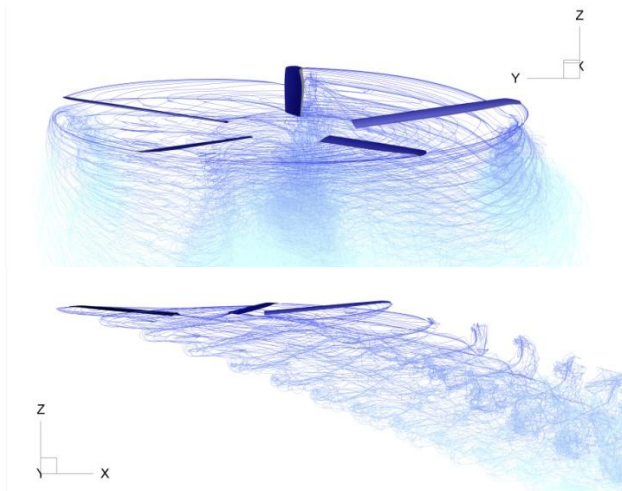


Figure 20. Isolated MR wake in TakeOff

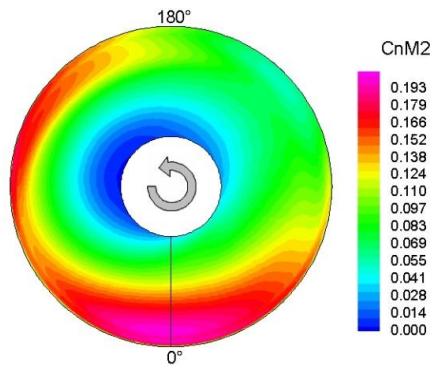


Figure 21. Contour plot of  $C_n M^2$  distribution on MR disk in TakeOff condition (last turn)

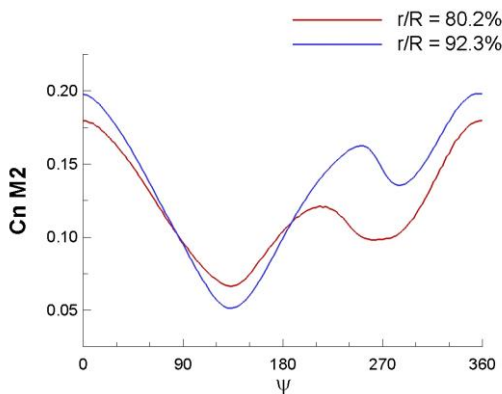


Figure 22.  $C_n M^2$  history for the isolated MR in TakeOff

### TR Aerodynamics (Isolated and Coupled)

In take-off the conceptual helicopter results to be much more affected by the MR/TR coupling than in flyover. The combination of trim state and MR wake path is such that the latter interacts with the TR blade mainly on the advancing side of the rotor disk (see Figure 23) causing stronger interactional phenomena. Contrary to flyover, in take-off it was found that, to ensure the same TR thrust force for anti-torque purposes, the pedal angle must be reduced of about  $1^\circ$  in case of MR/TR interaction with respect to the isolated TR. This confirms the subtleties associated with the TR performances when the MR effects are taken into account. Figure 25, Figure 26, and Figure 27, display the  $C_n M^2$  and  $d(C_n M^2)/d\Psi$  contours for the last turn of the isolated TR and

for the last five turns of the coupled TR, as well as the  $C_n M^2$  azimuth histories. Again, some important differences can be observed with respect to the flyover case when comparing the isolated (Figure 26 top-left) versus coupled solutions. In take-off, due to the very high MR torque and to the reduced anti-torque contribute operated by the vertical fin, the TR must produce a very high disk loading in order to balance the MR yaw-moment contribute. Very high induced velocities generated by the TR blades tip vortices blow away, on the port side, the TR wake from the disk plane. The isolated TR, thus, does not display any significant self-BVI phenomena apart from some weak self blade-wake interactions at the blade tip around  $\Psi=90^\circ$ . Coupling between MR and TR aerodynamics causes, instead, strong deformations of the TR wake and interactions between the TR blades with the MR tip vortices, giving rise to some induced BVIs mainly between  $\Psi=90^\circ$  and  $\Psi=180^\circ$  on the outer part of the advancing blade. A local orthogonal blade-wake interaction seems to occur in this disk region. Also the retreating side results to be affected by some low frequency load oscillations

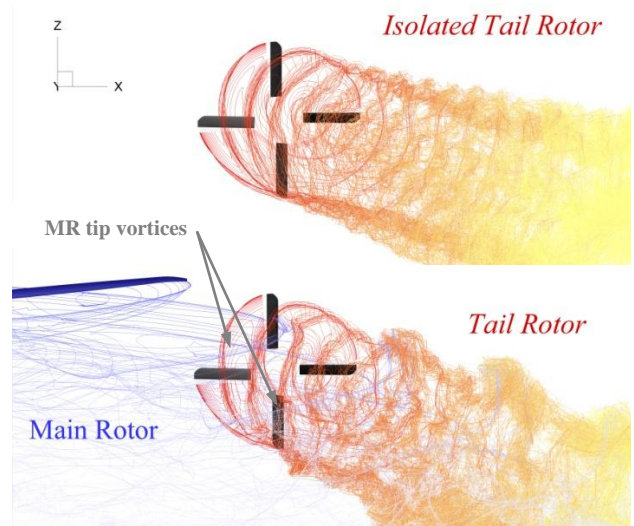


Figure 23. Isolated TR and coupled TR wake in TakeOff

(Figure 25, Figure 26, and Figure 27 moved on next page)

### Take-Off MR Acoustics (Isolated)

In Take-Off, MR mainly propagates on the starboard side and on the front of the disk. Like, in Flyover, MR hemisphere contour in dB(A) (see Figure 24) shows that its overall contribute is very low confirming that no high-frequency phenomena, such as self-BVI, occur.

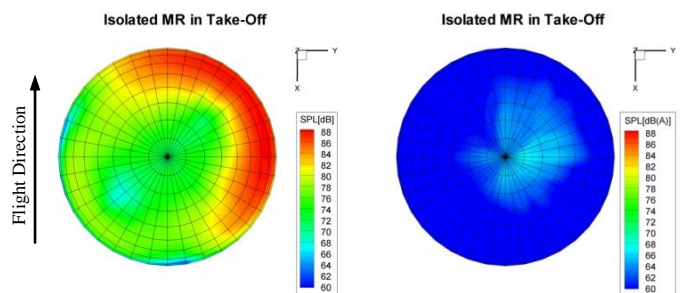


Figure 24 OASPL-dB and OASPL-dB(A) contours on the isolated MR hemisphere in Take-Off

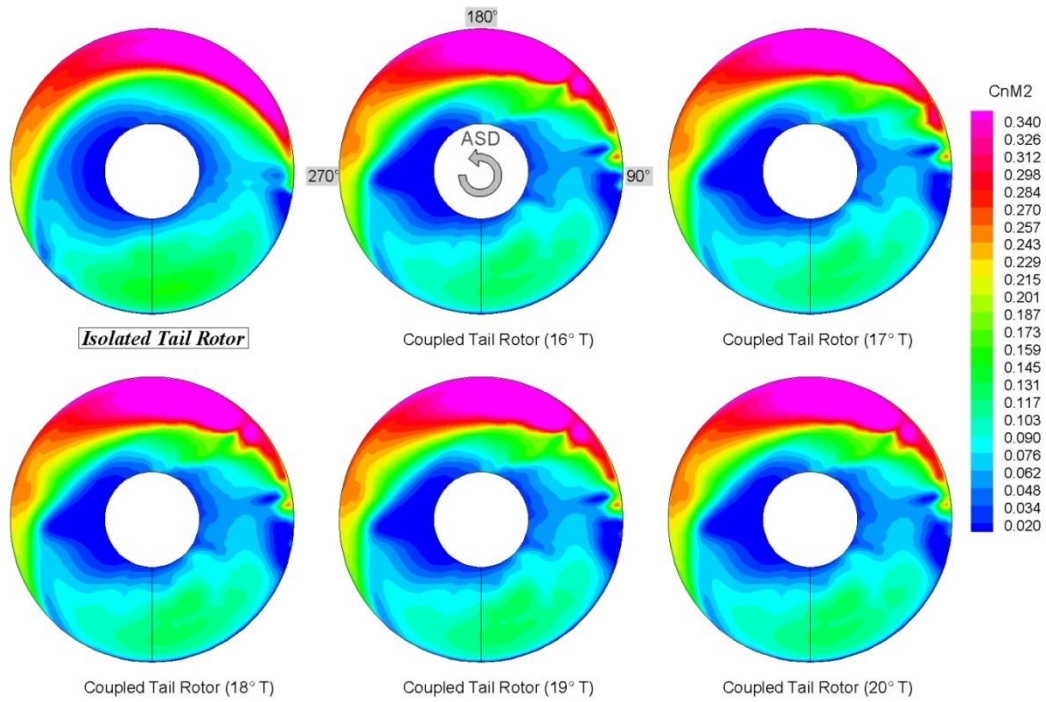


Figure 25. Contour plot of  $C_n M^2$  distribution on TR disk in TakeOff. Isolated TR (last turn) vs. Coupled TR (last five turns)

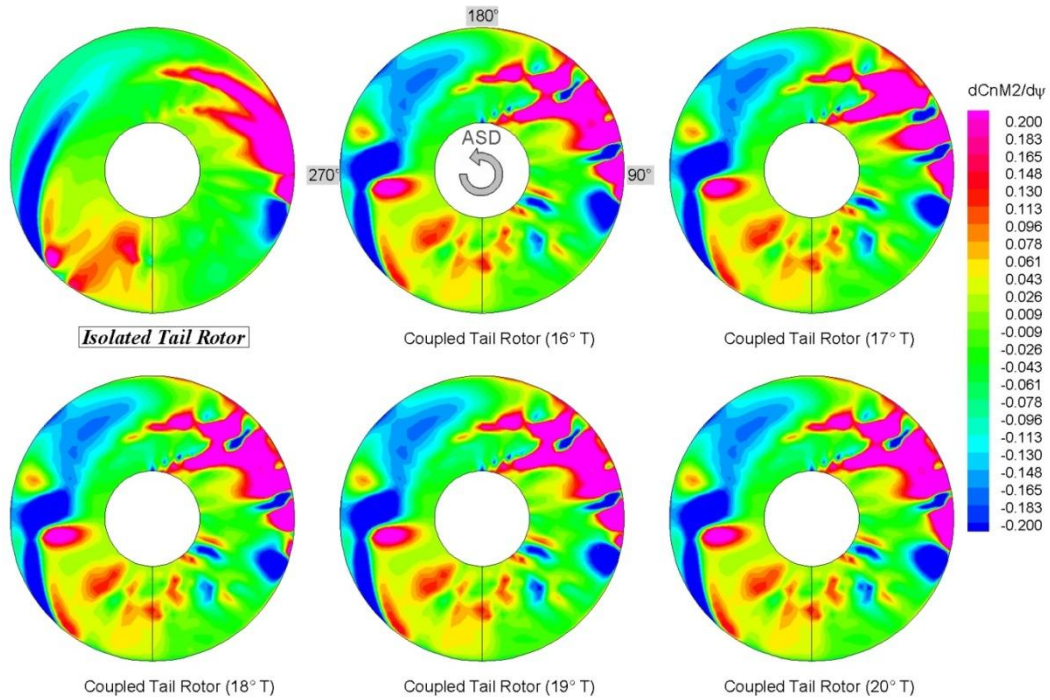


Figure 26. Contour plot of  $dC_n M^2/d\psi$  distribution on TR disk in TakeOff. Isolated TR (last turn) vs. Coupled TR (last five turns)

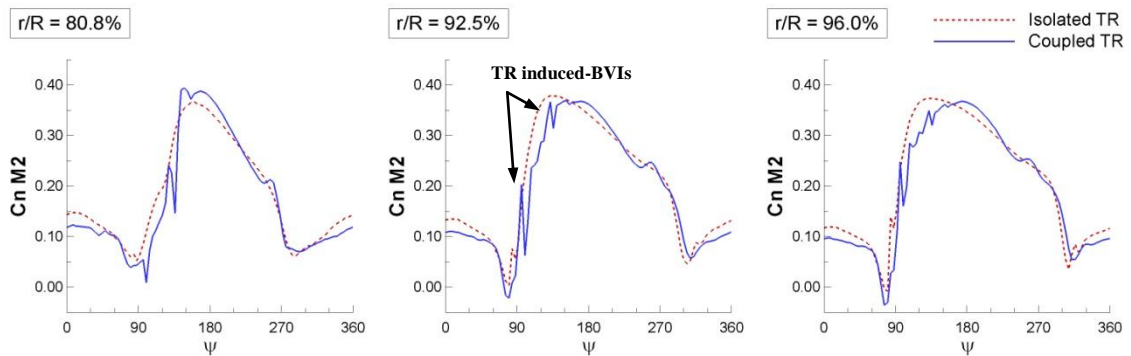


Figure 27. Sectional  $C_n M^2$  distributions comparison in TakeOff on last Tail rotor turn. Isolated TR (dashed) vs. Coupled TR (solid)

### Take-Off TR Acoustics (Isolated and Coupled)

Figure 28 shows the numerical hemispheres for both the isolated TR and for the TR under the interactional aerodynamics of the MR. TR directivity is mainly toward the port side of the helicopter and is affected by the 15° of TR cantilever angle. Contrary to Flyover, in Take-Off the interactional aerodynamic phenomena observed through Figure 23 to Figure 27 causes an increase in the noise levels for the coupled TR with respect to the isolated solution due to the MR-TR wake induced BVIs. Moreover, a slight change in directivity can be observed. Acoustic time histories for the points marked as “MAX” on the TR hemispheres are displayed, for one rotor revolution, in Figure 29. Along the whole rotor period, stronger BVI peaks, than the isolated TR, are visible.

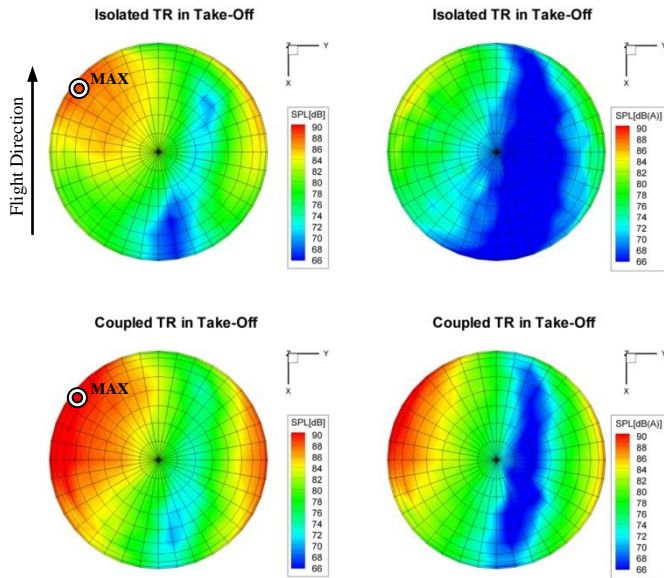


Figure 28 OASPL-dB and OASPL-dB(A) contours on the isolated and coupled TR hemispheres in Take-Off

TR acoustic frequency spectrum for the two points marked above as “MAX”, and displayed in Figure 30, confirms that, in Take-Off, the coupled TR displays higher SPL values than the isolated one. Again the interactional solution shows important noise contents not only at the rotor harmonics but also at intermediate frequencies. Due to the MR-TR wake interactions, the whole acoustic energy content of the interactional TR is spread more continuously all over the frequency spectrum than the isolated one.

### Take-Off On-Ground Propagation

ICAO rules prescribe that in Take-Off the helicopter is stabilized at the maximum take-off power and along a path starting from a point located 500m prior to the flight path reference point, at 20m above the ground, and at the best rate of climb speed. Then the take-off power is applied and a steady climb is initiated. The steady climb will be maintained throughout the 10-dB-down period and beyond the end of the certification flight path. Time history of the OASPL-dB for the certification central microphone, drawn in Figure 31 upper, shows that, in Take-Off, MR would be the major noise

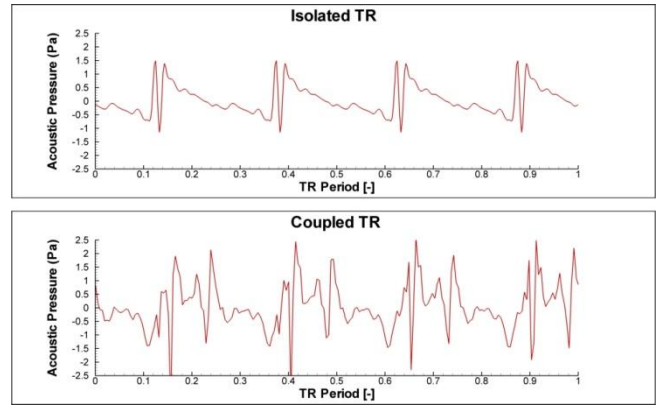


Figure 29 TR acoustic pressure time-histories for the points marked as “MAX” in Figure 28: isolated TR (upper) vs coupled TR (lower) in Take-Off

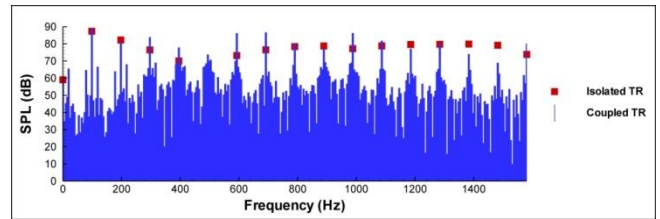


Figure 30 TR acoustic frequency spectrum in Take-Off for the points marked as “MAX” in Figure 28

contributor only at some distance from the microphone. This is a clear consequence of the different directivity pattern of MR and TR noise. When the helicopter is close to the microphone, the TR contribute is predominant. Contrary to flyover condition, in take-off it seems that no big differences exist between the isolated and the coupled TR OASPL-dB within the 10-dB-down period. When comparing the OASPL-dB(A) time histories (Figure 31 lower), instead, the MR+TR curves confirm again that the TR is the major noise source and that big differences arise between the interactional and isolated TR noise with a 4-dB(A) of delta. This different behaviour in terms of OASPL-dB and OASPL-dB(A) between flyover and take-off suggests that, while in flyover the isolated and coupled TR differ also at low frequencies, and thus, besides the OASPL-dB(A), the OASPL-dB is affected as well, in take-off the differences are confined only at high frequencies, i.e., only the dB(A) value is affected. The on-ground contour plots of the max OASPL-dB(A) for the sum of MR and TR (both isolated and coupled) are shown in Figure 32. Like in flyover, the EPNL value in take-off (Figure 33) confirms that the MR contribute is lower than the TR one and that the interactional TR contribute is more important than the isolated one.

### FLIGHT CONDITION 3: APPROACH

As in Take-Off, ICAO rules state that Approach must be performed at the best rate of climb speed ( $V_y = 80\text{kts}$  for the conceptual helicopter) while the descent path angle must be set to  $-6^\circ$ . In these flight conditions, the helicopter should suffer more than in other conditions of BVI phenomena.

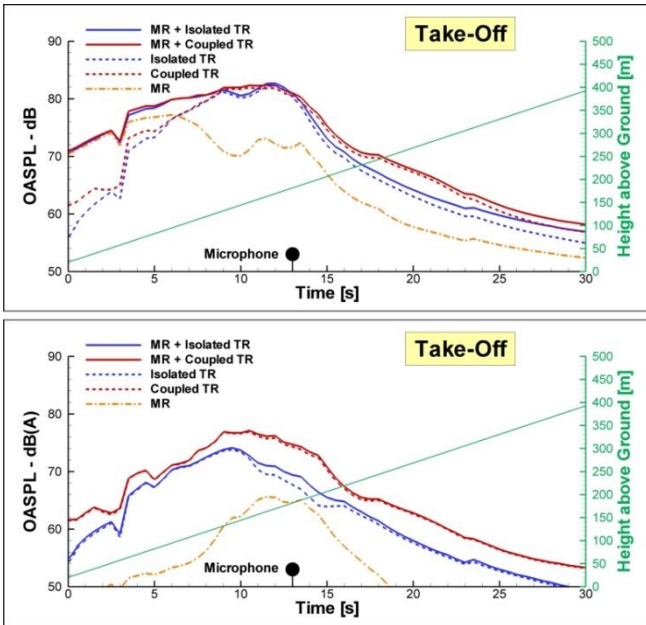


Figure 31 OASPL-dB and OASPL-dB(A) time-histories for the central microphone in Take-Off

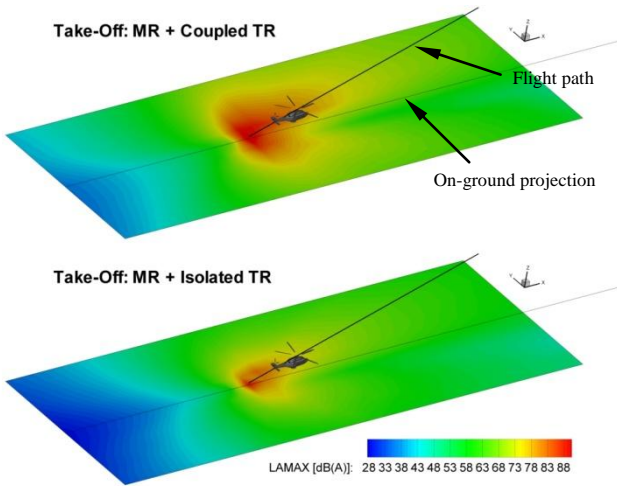


Figure 32 Max-OASPL-dB(A) contour plots in Take-Off: comparison between isolated and coupled TR

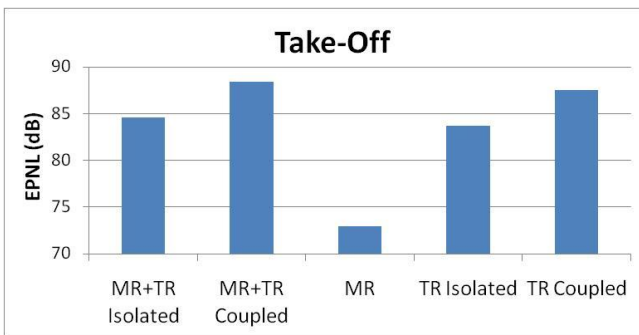


Figure 33 EPNL estimation in Take-Off

### MR Aerodynamics (Isolated)

In approach, due to the helicopter trim state and free stream velocity, the MR wake remains confined within the rotor disk causing the interaction between the blades and the tip vortices shed by the preceding ones, i.e., BVIs. Figure 34 clearly shows the relative position of the wake with respect to the rotor disk plane. Contrary to flyover and take-off, isolated

MR  $C_n M^2$  and  $dC_n M^2/d\Psi$  disk contours in approach (Figure 35) highlight the presence of sudden aerodynamic load fluctuations caused by parallel BVIs mainly around  $\Psi=45^\circ$  on the advancing side and around  $\Psi=300^\circ$  on the retreating side.  $C_n M^2$  time histories for two radial stations are drawn in Figure 36.

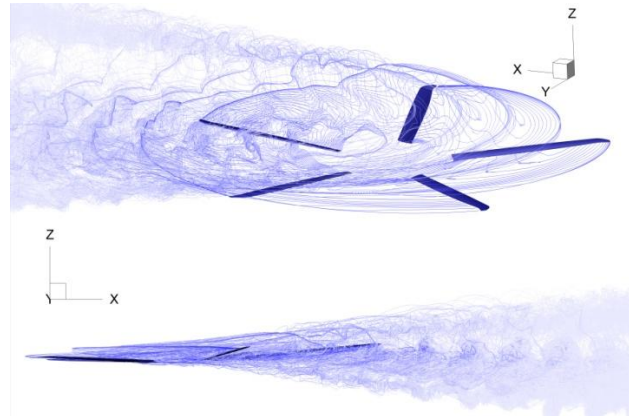


Figure 34. Isolated MR wake in Approach

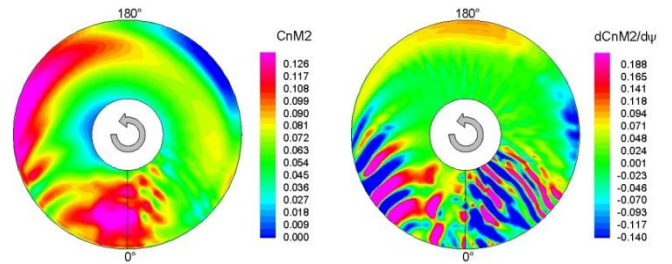


Figure 35 Contour plot of  $C_n M^2$  (left) and  $dC_n M^2/d\Psi$  (right) distributions on MR disk in Approach condition (last turn)

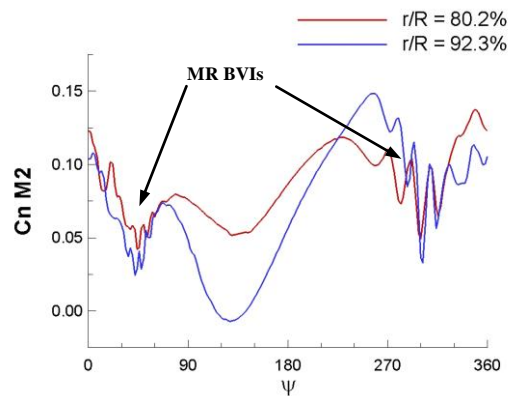


Figure 36.  $C_n M^2$  history for the isolated MR in Approach

### TR Aerodynamics (Isolated and Coupled)

Isolated TR  $C_n M^2$  (Figure 37) and  $dC_n M^2/d\Psi$  (Figure 38) disk contours show that the isolated TR exhibits stronger BVIs than the coupled solution. Like in flyover, the MR wake interacts in such a way to alter the load distribution reducing the BVIs on the advancing side while determining some interactions on the retreating one. Anyway, due to the very low TR disk loading, in approach, the MR-TR wake interaction results in a weaker coupling with respect to the

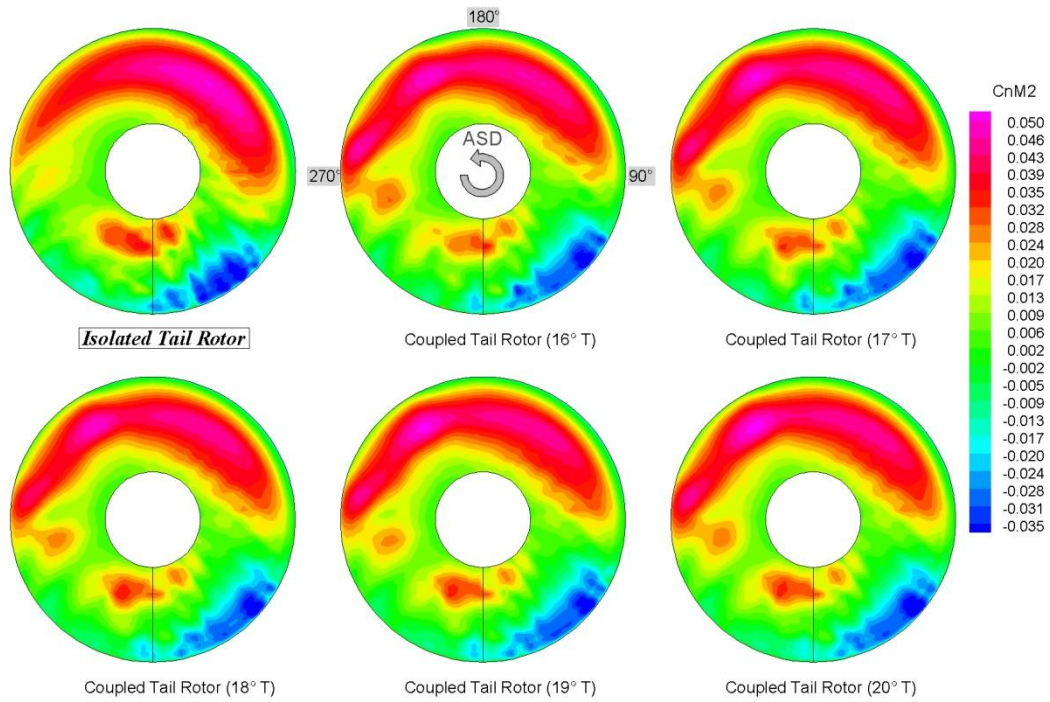


Figure 37. Contour plot of  $C_n M^2$  distribution on TR disk in Approach. Isolated TR (last turn) vs. Coupled TR (last five turns)

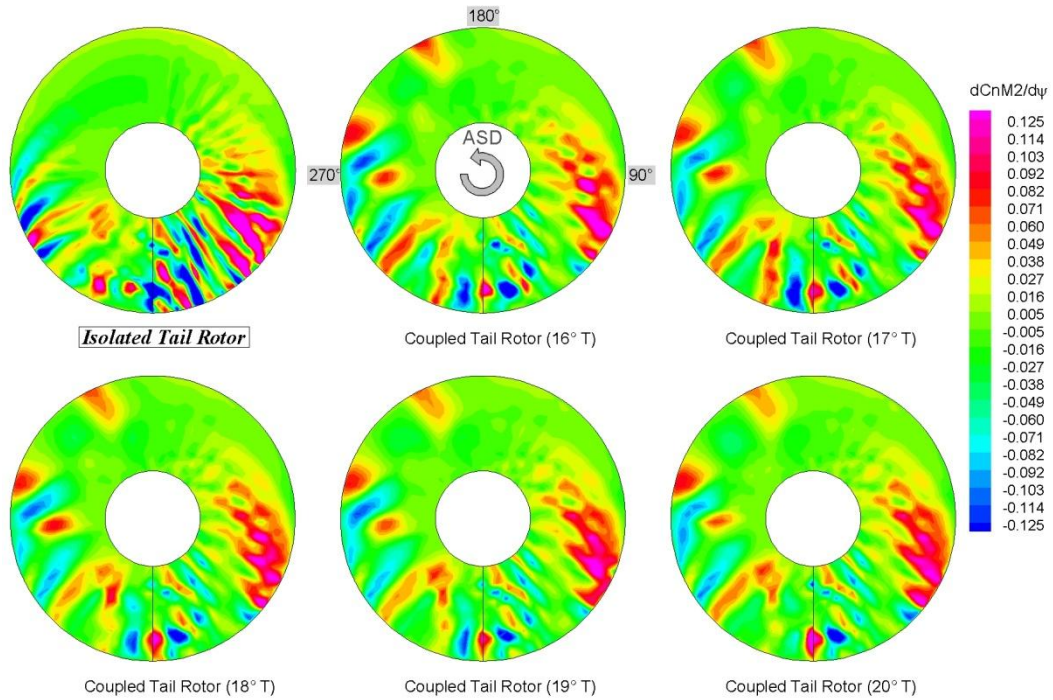


Figure 38. Contour plot of  $dC_n M^2/d\psi$  distribution on TR disk in Approach. Isolated TR (last turn) vs. Coupled TR (last five turns)

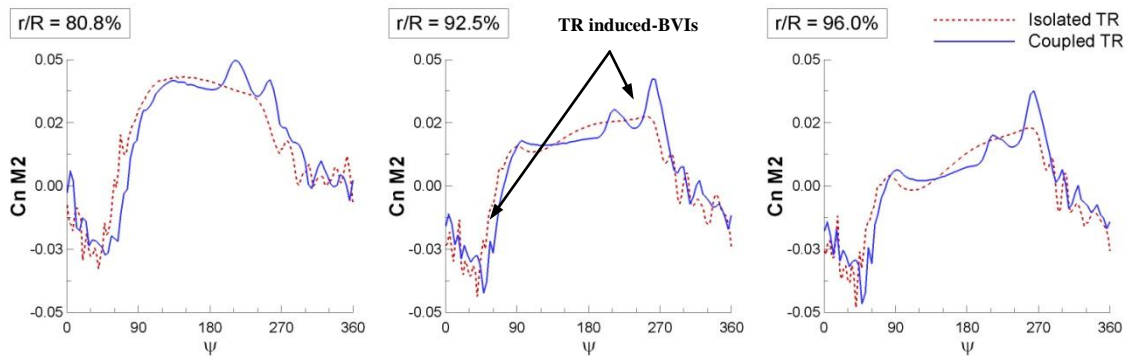


Figure 39. Sectional  $C_n M^2$  distributions comparison in Approach on last Tail rotor turn. Isolated TR (dashed) vs. Coupled TR (solid)

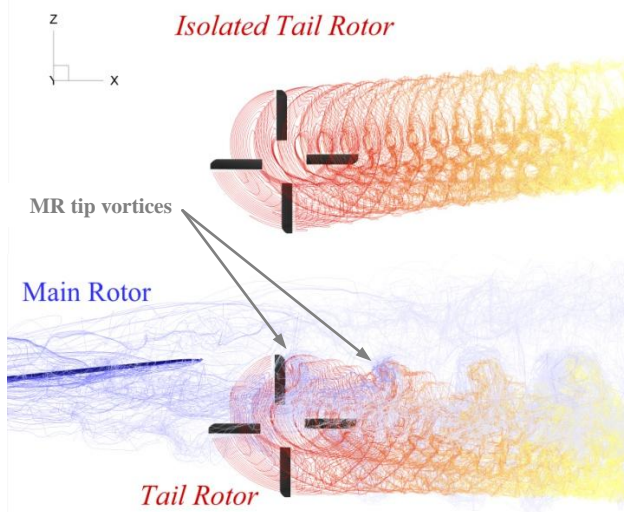


Figure 40. Isolated TR and interactional TR wake in Approach

flyover and take-off cases with very small or low frequency oscillations. MR wake interacts with the TR blades and wake mainly on the retreating side of the disk pushing downward the TR wake (Figure 40).

#### Approach MR Acoustics (Isolated)

In Approach MR acoustic is dominated, as expected, by mid-frequency BVIs propagating mainly on the starboard side of the rotor disk and displaying high levels of OASPL both in dB and dB(A) (see for instance Figure 41).

#### Approach TR Acoustics (Isolated and Coupled)

Figure 42 confirms that in approach the TR noise contribute is quite negligible if compared to the MR and that the impingement of the MR wake tends to reduce or cancel some of the weak self-BVI's occurring on the isolated TR solution.

#### Flyover On-Ground Propagation

Approach must be performed at the  $V_y$  speed, or the lowest approved for this manoeuvre, with a  $-6^\circ$  of flight path. The helicopter height above the reference point, i.e., where the central microphone is located, must be 120m. Both OASPL-dB and -dB(A) time histories (Figure 43) confirms that the interactional TR exhibits lower values compared to the isolated one but, more important, that the TR noise contribute is much lower than the MR one. The on-ground contour plots of the max OASPL-dB(A) for the sum of MR and TR (both isolated and coupled) are shown hereafter in Figure 44 while MR, TR, and MR+TR contribute to the final EPNL value are drawn in Figure 45.

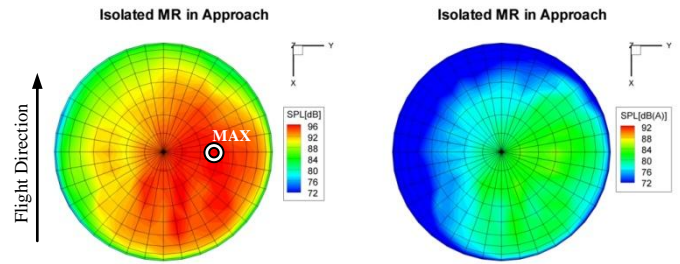


Figure 41 OASPL-dB and OASPL-dB(A) contours on the isolated MR hemisphere in Approach

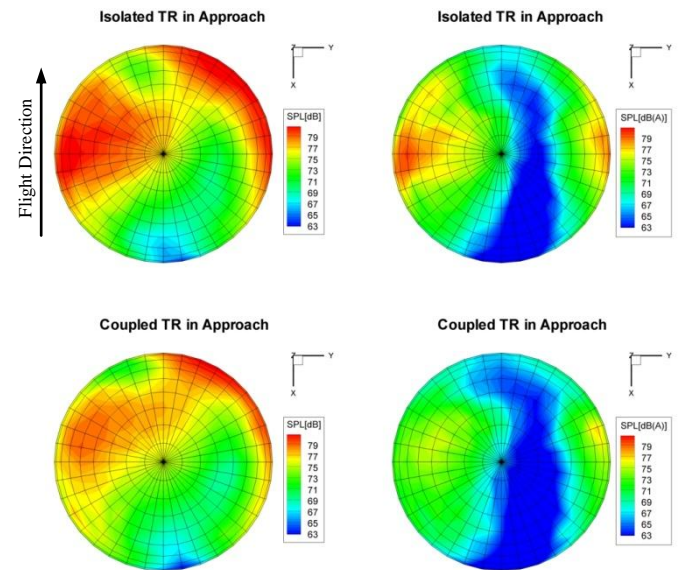


Figure 42 OASPL-dB and OASPL-dB(A) contours on the isolated and coupled TR hemispheres in Approach

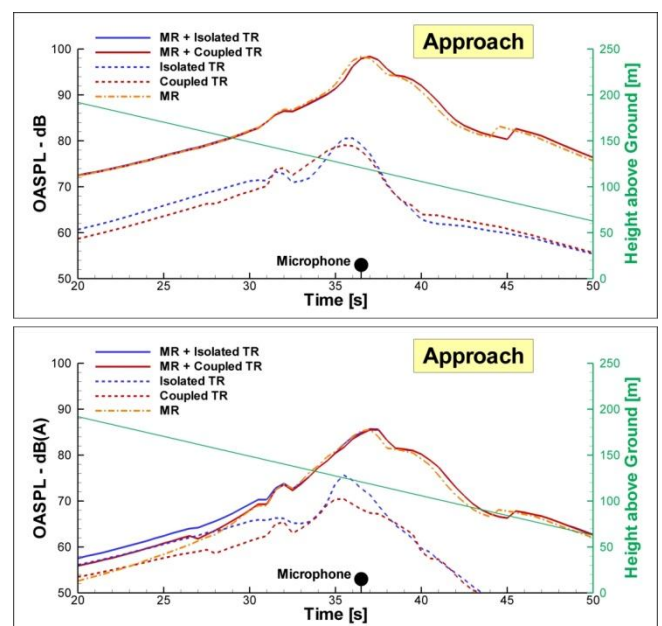
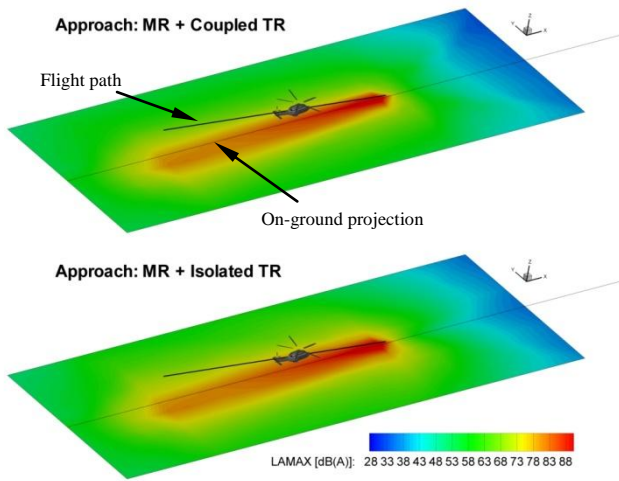
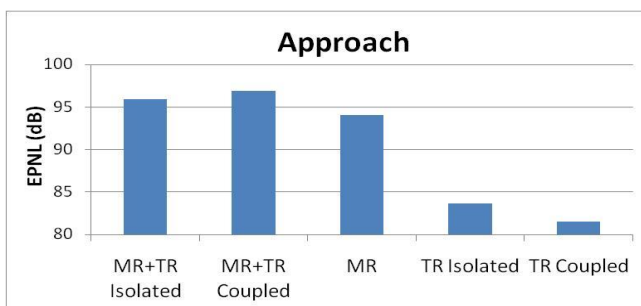


Figure 43 OASPL-dB and OASPL-dB(A) time-histories for the central microphone in Approach



**Figure 44 Max-OASPL-dB(A) contour plots in Approach: comparison between isolated and coupled TR**



**Figure 45 EPNL estimation in Approach**

## CONCLUSIONS

Even if the TR acoustics have been early recognized to be very important, very few numerical and experimental studies have been carried out in order to better understand its real involvement in the determination of the contribute to the whole helicopter's community annoyance. The complex aerodynamic environment in which the TR operates makes its aeroacoustic simulation very challenging but at the same time does not allow to figure out a general rule about the TR interactional aeroacoustic effects. The TR acoustics, indeed, is also strongly dependent on the helicopter configuration and trim parameters. The authors, in the present work, focused on the effects of MR and TR interactional aerodynamics, and related effects on the on-ground acoustic propagation, in three typical certification conditions for a medium-heavy conceptual helicopter: flyover, take-off, and approach. An advancing-side-down TR has been used. Flyover simulations demonstrated that TR is the major noise contributor to the helicopter noise if compared to the MR due to its high frequency contents. Moreover, interactional aeroacoustic simulations highlighted that the induced MR wake effects tend to modify the TR blade-wake interactions causing a reduction or partially cancellation of some of the strong self-BVIs occurring on a isolated TR. In take-off, instead, the MR wake strongly interact with the TR blades causing additional and stronger BVIs than the isolated configuration. Again, in take-off, the TR is the most important noise source if compared to the MR. Flyover and take-off results are also affected by the high TR disk loading. In approach, TR contribute to the overall helicopter noise is quite negligible and no important interactional effects can be observed.

## REFERENCES

- [1] <http://www.cleansky.eu>
- [2] Jones H.E., "A study of the Effects of Blade Shape on Rotor Noise", AHS Technical Specialists' Meeting for Rotorcraft acoustics and Aerodynamics, 1997
- [3] Hoad D.R., "Evaluation of Helicopter Noise Due to Blade-Vortex Interaction for Five Tip Configurations", NASA TP1608
- [4] HU H., Jordan L.A., Baeder J.D., "CFD Investigation of Double-Swept Blade in BVI Noise Reduction", 9th AIAA/CEAS Aeroacoustics Conference, Hilton Head, SC, 12-14 May 2003
- [5] Leverton, J.W., "Reduction of Helicopter Noise by Use of a Quiet Tail Rotor", Paper No. 24, European Rotorcraft Forum, Sept. 1980.
- [6] Edwards, B.D., Peryea, M.A. and Brieger, J.T. "1/5th Scale Model Studies of Main Rotor and Tail Rotor Interactions", Proceedings of the AHS National Specialist's Meeting on Aerodynamics and Aeroacoustics, Feb. 1987.
- [7] Fitzgerald, J. and Kohlepp, F., "Research Investigation of Helicopter Main Rotor/Tail Rotor Interaction Noise", NASA CR 4143, May 1988.
- [8] George, A. R., Chou, S. T., "Helicopter tail-rotor blade-vortex interaction noise", NASA-CR-183178, 1987
- [9] Yin J.P., Ahmed S.R., "Helicopter main-rotor/tail-rotor interaction", Journal of the American helicopter society, Vol.45, No.4, pp293-302, October 2000.
- [10] Yin J.P., "Simulation of Tail Rotor Noise Reduction and Comparison with HeliNovi Wind Tunnel Test Data", 67th AHS Annual Forum, May 3-5, 2011
- [11] Brown R.E., Fletcher T.M., Duraisamy K., "Sensitivity of Tail Rotor Noise to Helicopter Configuration in Forward Flight", 65th AHS Annual Forum, May 27-29, 2009.
- [12] Johnson, W., "Camrad/JA - A Comprehensive Analytical Model of Rotorcraft Aerodynamics and Dynamics - Volume II: User's Manual", Johnson Aeronautics, 1988.
- [13] D'Andrea, A., "Development of a Multi-Processor Unstructured Panel Code Coupled with a CVC Free Wake Model for Advanced Analyses of Rotorcrafts and Tiltrotors", 64th AHS Annual Forum, Montréal, Canada, Apr. 29-May 1, 2008
- [14] Ponza R., "Flying Helicopters Acoustic Impact Assessment: Towards a More Realistic Simulation Methodology", ECCOMAS 2004, 24-28 July 2004.
- [15] Tuinstra M., Duque Gerales C.M., "HELicopter Environmental Noise Analysis (HELENA) Software Tool", NLR-CR-2010-346
- [16] Gervais M., Gareton V., Dummel A., Heger R., "Validation of EC130 and EC135 Environmental Impact Assessment Using HELENA", 66th AHS Annual Forum, May 11-13, 2010.
- [17] Nannoni, F., Giancamilli, M., Cicalè, M., "ERICA: The European Advanced Tiltrotor", 27th European Rotorcraft Forum, September 11-14, 2001.
- [18] "Standard Values of Atmospheric Absorption as a Function of Temperature and Humidity", SAEARP 866A, 31/08/1964, Revised 15/03/1975
- [19] Zaporozhets O., Tokarev V., "Improving prediction models for noise footprint calculations in a part of sound propagation and installations effects in operating conditions", NAU (084-M02), Kyiv 2002